Urban Heat Island Amplification Estimates on Global Warming Using an Albedo Model

Alec Feinberg

Key Words: Urban Heat Islands, Albedo Modeling, UHI Amplification Effects, UHI Heat Dome, Cool Roofs, Sea Ice Warming

Abstract In this paper, we provide nominal and worst-case estimates of radiative forcing due to UHI effect using a Weighted Amplification Albedo Solar Urbanization (WAASU) model. This calculation is done with the help of reported findings from UHI footprint and heat dome studies that simplify estimates for UHI amplification factors. Using this method, we quantify a global warming range due to the UHI effect (including urban coverage). Variations in our estimates are due to urbanized area assessments and amplification factor uncertainties. However, the model showed consistent estimates of about 0.155W/m^2/%normalized effective amplified area for the urbanized area forcing value. Significance increase when the UHI effective contribution to climate feedback estimates are included. The basic model is additionally used to quantify warming due to sea ice loss in assessing related feedback temperature rises. Results provide insight into the UHI area effects from a new perspective using a global view albedo model compared to prior ground based studies. It also illustrates the utility of using effective UHI amplification factors when assessing UHI's warming effect on a global scale.

1 Introduction

There are few recent publications about possible UHI influences on global warming, more up-to-date related studies, including UHI amplification effects that will be discussed in this paper, could offer supporting data for climate change theories and solutions. One key paper often referred to is by McKitrick and Michaels [1,2] who found that the net warming bias at the global level may explain as much as half the observed land-based warming. This study was criticized by Schmidt [3] and defended by Mckitrick [2] over many years. Other authors have also found significance [4-12]. These studies used land-based temperature station data to make assessments. In our study, where we introduce a Weighted Amplification Albedo Solar Urbanization (WAASU) model, we will see it has some advantages as it works from a global view rather than these ground based studies. We also show its utility by extending it to a Weighted Albedo Solar (WAS) model for global warming estimates due to Arctic ice melting. This helps in determining related feedback temperature rise assessments due to the UHI effect which is an enhanced advantage of this type of modeling. The model is non-probabilistic and in line with typical energy budgets (IPCC, Hartmann et al. [13]). It uses only two key parameters: normalized effective amplified area and average albedo. Because it is simplistic, it has transparency compared with the complex land-based studies.

The contention that UHI effects are basically only of local significance is most likely related to urban area estimates. For example, the IPCC (Satterthwaite et. al. [14]) AR5 report references a Schneider et al. [15] study that resulted in urban coverage of 0.148% of the Earth (Table 1). This seemingly small area tends to dismiss the role that the UHI effect can play in large-scale global warming. Furthermore, estimates of how much land has been urbanized vary widely in the literature, in part due to the definition of what is urban and the datasets used. Although, such estimates are important for environmental studies, obtaining true estimates for the small urbanized area relative to the total land is apparently very difficult. Compounded by the fact that there is a significant difference in how groups define the term "urban". Table 1 illustrates a number of variations from select papers of interest.

In addition, global warming UHI amplification effects have not been quantified to a large degree related to area estimates. Urbanized average solar areas remain unknown.

Table 1. Urbanization area extent estimates from various sources

Percent of Land	Percent of Earth	References
2.7	0.783	GRUMP [16] – using NASA satellite light studies based on 2004 data and supplemented with census data
1	0.29	NASA [17], Galka [18] – from satellite data
0.51	0.148	Schneider et al. [15] – based on 2000-2001 data and referenced in the IPCC report (Satterthwaite, [14])
0.5	0.145	Zhou [19] – based on a 2000 data set

In our study, one key paper listed in Table 1 is due to Schneider et al. [15] since it is cited by the AR5 2014 IPCC report (Satterthwaite et al. [14]). In Schneider's paper, the larger area found in the GRUMP [16] study (Table 1) is criticized.

A. Feinberg, Ph.D., DfRSoft Research, email: dfrsoft@gmail.com, ORCID: 0000-0003-4364-2460

These area estimates are of interest in our paper for the WAASU model. Additionally, the amplification factors we use are related to their urban coverage estimates.

In this paper we use both the Schneider et al. and GRUMP studies for the nominal and worst-cases urbanization area estimates respectively. Furthermore, they were both done using data sets near the year 2000, a good point in time to extrapolate down to 1950 and up to 2019 (see Sec. 2.5).

1.1 UHI Amplification Effects

The table below lists key global warming causes and amplification effects. In this section we will summarize only the UHI amplification effects listed in the table since the root-causes and the main global warming feedback amplification effects are fairly well known.

Table 2. Global warming cause and effects

Global Warming Causes →	Population → Expanding Urban Heat Islands (UHI), Roads & Increases in Greenhouse Gas
Global Warming Feedback Amplification Effects →	Water-Vapor Feedback, Land Albedo Change Due to Cities & Roads, Ice and Snow –Albedo Feedback, Lapse Rate Feedback, Cloud Feedback, etc.
Urban Heat Island Amplification Effects →	UHI Solar Heating Area (Building Areas), UHI Building Heat Capacities, Humidity Effects and Hydro-Hotspots, Reduced Wind Cooling, Solar Canyons, Loss of Wetlands, Increase in Impermeable Surfaces, Loss of Evapotranspiration Natural Cooling.

The UHI amplification effects that we consider to dominate listed in the table are as follows:

- ***The humidity amplification effect:*** This effect has been observed. For example, Zhao et al. [20] noted that UHI temperature increases in daytime ΔT by 3.0°C in humid climates but decreasing ΔT by 1.5°C in dry climates. They noted that such relationships imply UHIs will exacerbate heat wave stress on human health in wet UHI climates. One explanation is how heat dissipates through convection which is more difficult in humid climates. Another explanation is that warmer air holds more water-vapor. This can increase local specific humidity so that there could be local greenhouse effects.

- ***The heat capacity and solar heating area amplification effect:*** This effect contributes to the day-night UHI cycle. In most cities, it is observed that daytime atmospheric temperatures are actually cooler compared to night. For example, in a study by Basara et al. [21] in Oklahoma city UHI, it was found that at just 9-m height, the UHI was consistently 0.5–1.75°C greater in the urban core than the surrounding rural locations at night. Further, in general UHI impact was strongest during the overnight hours and weakest during the day. This inversion effect can be the result of massive UHI buildings acting like heat sinks, having giant heat capacities and storing heat in their reservoir via convection as solar radiation is absorbed during the day. This occurrence often reduces the UHI day effect, but at night buildings cool down, giving off their stored heat that increases local temperatures to the surrounding atmosphere. This effect increases with city growth as buildings have gotten substantially taller since 1950 (Barr [22]).

- ***The hydro-hotspot amplification effect:*** This effect is not well addressed. Atmospheric moisture source is a complex issue due to Hydro-HotSpots (HHS). HHS occurs when buildings are hot due to sun exposure. Then, during precipitation periods, the hot evaporation surfaces increase localized water-vapor as warm air holds more moisture. This increase in local greenhouse gas could blanket city heat and increase infrared radiation during these periods, providing another UHI humidity amplification source.

- ***Reduced wind cooling and solar canyons:*** In UHIs reduced wind is a known effect due to building wind friction that inhibits cooling by convection. Tall buildings also create solar canyons and trap sunlight, reducing the average albedo, although some benefits occur from shading. In general, both have the effect of amplifying the temperature profile of UHIs.

2 Data and Methods

We see from the previous section that estimating climate change impact just based on the UHI area coverage as in Table 1, does not take into account of the effects of solar heating building sidewall areas, massive heat capacities, humidity issues, wind reduction and the solar canyon trapping that collectively amplify UHI effects beyond its own climate area.

2.1 UHI Area Amplification Factor

To estimate the UHI amplification effects, it is logical to first look at UHI footprint (FP) studies as they provide some measurement information. Zhang et al. [23] found the ecological FP of urban land cover extends beyond the perimeter of urban areas, and the FP of urban climates on vegetation phenology they found was 2.4 times the size of the actual urban land cover. In a more recent study by Zhou et al. [24], they looked at day-night cycles using temperature difference measurements in China. In this study, they found UHI effect decayed exponentially toward rural areas for the majority of the 32 Chinese cities. Their comprehensive study spanned from 2003 to 2012. They describe China as an ideal area to study since it has experienced the most rapid urbanization in the world in the decade they evaluated. They found that the FP of UHI effect, including urban areas, was 2.3 and 3.9 times that of urban size for the day and night, respectively. We note that the average day-night amplification footprint coverage factor is 3.1.

Looking at Table 2, we see that the UHI Amplification Factor (AF) is highly complex making it difficult to assess from first principles as it would be some function of Table 2 components relative to a reference year:

$$AF_{UHI\ for\ 2019} = f\left(\overline{Build}_{Area}\ x\ \overline{Build}_{C_p}\ x\ \overline{R}_{wind}\ x\ \overline{LossE}_{vtr}\ x\ \overline{Hy}\ x\ \overline{S}_{canyon}\right) \tag{1}$$

were

$\overline{Build}_{Area}$ =Average building solar area
$\overline{Build}_{C_p}$ = Average building heat capacity
$\overline{R}_{wind}$ = Average city wind resistance
$\overline{LossE}_{vtr}$ = Average loss of evapotranspiration to natural cooling & loss of wetland
$\overline{Hy}$ = Average humidity effect due to hydro-hotspot
$\overline{S}_{canyon}$ = Average solar canyon effect

To provide some estimate of this factor, we note that Zhou et al. [24] found the FP physical area (km^2), correlated tightly and positively with actual urban size having a correlation coefficients higher than 79%. This correlation can be used to provide an initial estimate of this complex factor. Therefore, as a model assumption, it seems reasonable to use area ratios for this estimate.

$$AF_{UHI\ for\ 2019} = \frac{\sum\left(UHI\ Area\right)_{2019}}{\sum\left(UHI\ Area\right)_{1950}} \tag{3}$$

Area estimates have been obtained in the next Section in Table 3 between 2019 and 1950 time frames, yielding the following results for the Schneider et al. [15] and the GRUMP [16] extrapolated area results:

$$AF_{UHI\ for\ 2019} = \frac{\left(Urban\ Size\right)_{2019}}{\left(Urban\ Size\right)_{1950}} \approx \begin{cases} \left(\dfrac{\left[0.188\right]_{2019}}{\left[0.059\right]_{1950}}\right)_{\text{Schneider}} = 3.19 \\ \left(\dfrac{\left[0.952\right]_{2019}}{\left[0.316\right]_{1950}}\right)_{GRUMP} = 3.0 \end{cases} \tag{3}$$

Between the two studies, the UHI area amplification factor average is 3.1. Coincidently, this factor is the same observed in the Zhou et al. [24] study for the average footprint. This factor may seem high. However, it is likely conservative as other effects would be difficult to assess: increases in global drought due to loss of wet-lands, deforestation effects due to urbanization, and drought related fires. It could also be important to factor in changes of other impermeable surfaces since 1950, such as highways, parking lots, event centers, and so forth.

The area amplification value of 3.1 is then considered as one of our model assumptions.

2.2 Alternate Method Using the UHI's Dome Extent

An alternate approach to check the estimate of Equation 3, is to look at the UHI's dome extent. Fan et al. [25] using an energy balance model to obtain the maximum horizontal extent of a UHI heat dome in numerous urban areas found the nighttime extent of 1.5 to 3.5 times the diameter of the city's urban area (2.5 average) and the daytime value of 2.0 to 3.3 (2.65 average).

Applying this energy method (instead of the area ratio factor in Eq. 3, yields a diameter in 2019 compared to that of 1950 with an increase of 1.8. This method implies a factor of 2.5 x 1.8=4.5 higher in the night and 2.65 x 1.8=4.8 in the day in 1950 with an average 4.65. This increase occurs 62.5% of the time according to Fan et al., where their steady state occurred about 4 hours after sunrise and 5 hours after sunset yielding an effective UHI amplification factor of 2.9. We note this amplification factor is in good agreement with Equation 3. Fan et al. [25] assessed the heat flux over the urban area extent to its neighboring rural area where the air is transported from the urban heat dome flow. Therefore the heat dome extends in a similar manner as observed in the footprint studies. If we use the dome concept, we can make an assumption that the actual surface area for the heat flux is increased by the surface area of the dome. We actually do not know the true diameter of the dome, but it is larger than the assessment by Fan et al.. Using the dome extend due to Fan et al. [25] applied to the area of diameter D, the amplification factor should be correlated to the ratios of the dome surface areas:

$$AF_{UHI\ for\ 2019} = \left(\frac{D_{2019}}{D_{1950}} \right)^2 = 2.9^2 = 8.4 \tag{4}$$

Thus, this equation is our second model assumption, where it is reasonable to use the ratios of the dome's surface area for an alternate approach in estimating the effective UHI amplification factor. We will have two values, 3.1 and 8.4 to work with that will help in assessing model consistency and provide upper and lower bounds for effective amplification area.

2.3 Applying the Amplification Factors

In this analysis, 1950 is the reference year. Therefore it is not subjected to amplification. Only the new area is amplified as we are looking at changes since this time frame. This is denoted as the Amplified Affected Area (AAA). The AAA in 2019 is then given by

$$AAA_{UHI\ for\ 2019} = AF(new\ area) + Area_{1950} = AF(Area_{2019} - Area_{1950}) + Area_{1950} \tag{5}$$

Using this, if there were no changes in UHI growth, for example so that the $Area_{2019}$=$Area_{1950}$, the resulting area is just the original $Area_{1950}$.This result is applied to the new area in Table 3 below.

2.4 Area Extrapolations for 1950 and 2019

To assess the urbanized area, (also used in determining the UHI amplification factor ratios above), we need to project the Schneider [15] and GRUMP [16] area estimates down to 1950 and up to 2019. Both use datasets are near to 2000, so this is a convenient somewhat middle time-frame. Here we decided to use the world population growth rate (World Bank [26]) which varies by year as shown in Appendix A in Figure A1. We used the average growth rate per ½ decade for iterative projections of about 1.3% to 1.6% per year.

To justify this projection, we see that Figure A2a illustrates that building material aggregates (USGS [27]) used to build cities and roads correlates well to population growth (USGS Population Growth [28]).

It is also interesting to note that building materials for cities and roads also correlates well to global warming trends (NASA [29]) shown in Figure A2b.

Column 2 in Table 3 shows the projections with the actual year (~2000) data point tabulated value also listed in the table (see also Table 1). The UHI area amplification factors (Column 3) is then applied to Schneider [15] and GRUMP [16] studies shown in Column 4 using Equation 5.

Table 3. Extrapolated and amplified urbanized coverage estimates

Year	Urban coverage percent of Earth	Amplification factor effect	Amplification Affected Area (AAA)
Schneider study [15]			
1950	0.059*	1	**0.059%**
2000-2001	0.0051x29%=0.148		
2019	0.188*	3.1 AF_{Area}**	**0.459%**
2019	0.188*	8.4 AF_{Dome}**	**1.143%**
Worst-case GRUMP study [16]			
1950	0.316%*	1	**0.316%**
2000	0.027x29%=0.783%		
2019	0.952%*	3.1 AF_{UHI}**	**2.288%**
2019	0.952%*	8.4 AF_{Dome}**	**5.658%**

*Growth rate of cities using world population yearly growth rate in Fig A1, **AF_{UHI} is the area amplification factor for 2019 referenced to 1950.

2.5 Weighted Amplification Albedo Solar Urbanization (WAASU) Model Overview

The WAASU model is very straightforward; it is based on a global weighted albedo model. The Earth Albedo is given by

$$Earth\ Albedo = \sum_i \{\%\, Effective\ SurfaceArea_i\ x\ Surface\ Item\ Albedo_i\} + Cloud\ Area\ x\ Cloud\ Albedo. \quad (6)$$

Here the effective surface area is given by

$$Effective\ SurfaceArea = Surface\ Area\ x\ \%Solar\ Irradiance. \quad (7)$$

where the surface area includes all areas including AAA. We note that the change in the Earth Albedo over time (from 1950 to 2019), is just a function of the UHI area variation, (when holding all unrelated UHI components constant), that is

$$\left(\frac{dEA}{dt}\right)_{EA'} = \sum\left(Albedo_{UHI}\ x\ \%Solar\ Irradiance\ x\ \frac{dSurfaceArea_{UHI}}{dt}\right)_i, \quad (8)$$

where EA is the Earth's albedo (Eq. 6 and 7), and EA' is all other Earth components (held constant). Although it is possible that the solar irradiance percent changes due to new city locations, in this model we assume it is fixed at 100%. This indicates, for example, that even if we were to change the *effective Surface Area* of perhaps the *sea ice component* because it receives about 40% irradiance compared with other areas and redistributed its radiance (per the Earth's energy budget), it would not affect the overall results when looking at the albedo change over time due to the UHI effect from 1950 to 2019. Therefore, the model only requires we work with normalized area coverage changes when focusing solely on the UHI effect. On the other hand, solar irradiance comes into play for sea ice when we are considering its global albedo effect from 1950 to 2019 (see Appendix C). However, the solar radiation weighting, albedo, and areas for all Earth components are subjected to the constraints below.

2.5.1 Model Constraints

This model is subject to the constraint

$$Total\ Area = \sum_i \{\%\, Normalized\ Effective\ Amplified\ SurfaceAreas_i\} + \%Cloud\ Area = 100\% \quad (9)$$

and the normalization effective amplified area (NEAA) constraint for the Earth surface areas (when the UHI area is increased) must then be subject to

$$\sum_i \{\%\, Normalized\ Effective\ Amplified\ Surface\ Areas_i\} = 100\% - \%Cloud\ Area. \quad (10)$$

To simplify things as much as possible, ***only five Earth constituents are used:*** *water, sea ice, land, UHI coverage, and clouds* (where *land* is its area minus the UHI coverage). These components are fairly easy to estimate and references for their values are provided in Appendix D. Furthermore, we use consistent values found in the IPCC AR5 report (Hartmann et al. [13]) assessment of the Earth's energy budget for solar irradiance. Table 4 summarizes the constraints from these IPCC values.

Table 4. IPCC Earth energy budget values (Hartmann et al. [13])

IPCC Item	Incident and Reflected Radiation (W/m^2)	Albedo %	Absorbed (W/m^2)
Earth	100/340	**29.4118**	240=340x(1-.294)
Atmosphere & Clouds	76/340	**22.3529**	**79**
Earth Surface Albedo	24/340	**7.0588**	**161**

The fixed components of our model maintain relative consistency from 1950 to 2019. The non-fixed value is the urban coverage as indicated by Equation 8. The only unknown value is the *land* albedo (minus the UHI coverage) and this value is adjusted to obtain the IPCC global albedo, 29.4118% and its *land* value of incident/reflected value of 7.0588.

These values are used as a 1950 starting point and then the 2019 increase for UHI coverage area is inserted. This increases the Earth's area to greater than 100%. Therefore, renormalization is done per the constraint of Equation 10. Renormalization is detailed in Appendix B.

3 Results and Discussion

Using the extrapolated area coverage in Table 3 with the 3.1 amplification factor applied to the urbanized growth, the resulting global albedo change occurred of 29.3956% in 2019 (Table 5b) compared to the earlier 1950 albedo value of 29.4118% (Table 5a) for the Schneider nominal case. As well, for the GRUMP worst-case, the albedo changed from 29.4118% (Table 6a) to 29.3322% (Table 6b) due to the urbanized growth**.** Dome values are also listed in the Table and for the Schneider case results are in Appendix B, Table B2.

As we mentioned earlier, the increases in the solar surface area of the Earth, which will occur with city growth of tall buildings and their solar areas, however comparatively small, requires renormalization in the model of the Earth surface components of the WAASU model (detailed in Appendix B). This information is displayed in Column 3 in Tables 5b,6b and B2. While the model is sensitive to urban coverage changes, it works well with renormalization showing a high level of consistency to urban coverage proportionality changes. This consistency is indicated in Table 7 where we find the GRUMP [16] area **forcing** is 0.0944% (W/m^2)/Norm Area (=0.271/2.87) compared with the Schneider area **forcing** of 0.0948 (W/m^2)/ %Norm Area (=0.055/0.58).

Table 7 provides a summary of albedo changes found in the WASSU model along with the expected solar long wave radiation increase. From the above global WAASU model, the estimates of the Earth's radiated long wavelength emissions are set equal to the short wave radiation absorption:

$$P_\alpha = 340\ W/m^2\ (1\text{-Albedo}). \quad (11)$$

Then the albedo change from 1950 to 2019 represents the equivalent increase in long wave radiation is given by

$$\Delta P_\alpha = 340\ W/m^2\ \{(1\text{-Albedo})_{2019} - (1\text{-Albedo})_{1950}\}. \quad (12)$$

Table 5a. Schneider results (Albedo=29.4118, 1950)

Surface	Albedo	% Area of Surface	Normalized Earth Area	Weighted Albedo %
	A	B	C=A x B x (1-0.67)	A x C
Sum of Water Type		71		
Sea Ice	0.6	15	4.95	2.970
Water	0.06	56	18.48	1.109
Sum of Land Type		29		
Land - (UHI + Coverage)	0.3118	28.941	9.55053	2.978
UHI + Coverage	0.12	0.059	0.01947	0.002
		∑=100.000	33.000	7.05882
			Cloud Area	
Clouds	0.3336	67	67	22.35294
∑ Sum Earth %			100.000	
∑ Global Albedo				29.4118

Table 5b. Schneider results (Albedo=29.3956%, 2019)

Surface	Albedo	Normalized % Surface Area	Normalized Earth Area	Weighted Albedo %
	A	B	C=A x B x (1-0.67)	A x C
Sum of Water Type		70.717		
Sea Ice	0.6	14.94	4.9302	2.958
Water	0.06	55.777	18.406	1.1044
Sum of Land Type		29.283		
Land - (UHI + Coverage)	0.3118	28.826	9.513	2.966
UHI + Coverage	0.12	0.4571	0.1508	0.0181
		∑=100.000	33.000	7.0283
			Cloud Area	
Clouds	0.3336	67	67	22.3530
∑ Sum Earth %			100.000	
∑ Global Albedo				29.3994

Table 6a. GRUMP results (Albedo=29.4118, 1950)

Surface	Albedo	% Surface Area	Normalized Earth Area	Weighted Albedo %
	A	B	C=A x B x (1-0.67)	A x C
Sum of Water Type		71		
Sea Ice	0.6	15	4.95	2.970
Water	0.06	56	18.48	1.109
Sum of Land Type		29		
Land - (UHI + Coverage)	0.3135	28.684	9.46572	2.968
UHI + Coverage	0.12	0.316	0.10428	0.013
Sum Surface %		∑=100.000	33.000	7.0588
			Cloud Area	
Clouds	0.3336	67	67	22.3529
∑Sum Earth %			100.000	
∑ Global Albedo				29.4118

Table 6b. GRUMP results (Albedo=29.3322%, 2019)

Surface	Albedo	Normalized % Surface Area	Normalized Earth Area	Weighted Albedo %
	A	B	C=A x B x (1-0.67)	A x C
Sum of Water Type		69.627		
Sea Ice	0.6	14.71	4.8543	2.913
Water	0.06	54.917	18.12261	1.087
Sum of Land Type		30.3727		
Land - (UHI + Coverage)	0.3135	28.129	9.28257	2.910
UHI + Coverage	0.12	2.2437	0.740421	0.089
Sum Earth %		∑=100.000	33.000	6.9100
			Cloud Area	
Clouds	0.3336	67	67	22.3530
∑ Sum Earth %			100.000	
∑ Global Albedo				29.3519

Results are compiled in Table 7. The table also includes "what if" estimates, if we could change urbanization to be more reflective with cool roofs to reverse the effect.

The overall results (not including feedback effects) are summarized:

- Schneider nominal case from 1950 to 2019, the increase in LWR (Row 7) is 0.042W/m^2 and 0.113W/m^2 due to urban area and dome amplification coverage respectively. ~~These figures equate to about 1.18% and 3.2% of global warming assuming the total increase from 1950 is about 0.95°C in 2019~~.
- GRUMP worst-case from 1950 to 2019 the increase in LWR (Row 7) is 0.204W/m^2 and 0.537W/m^2 due to urban area and dome amplification coverage respectively. ~~This roughly equates to 5.7 and 15% of global warming assuming the total increase from 1950 is about 0.95°C in 2019.~~
- We note the consistency of the area forcing parameter having quite small variability and averaging about 0.155 *W/m^2/ %Normalized Effective Amplified Area (%NEAA)* and an average albedo forcing value of 5.4 *W/m^2/Global Albedo* change for the increase in LWR.
- We find in all cases, a value of 1W/m^2/%Δalbedo, which is likely a useful number. However, in assessment, it simplifies and is related to the expression with reference values 0.294118/100% x 340W/m^2.
- "What if" corrective action results of cool roofs indicates that changing city albedos in both the Schneider and the GRUMP case from 0.12 to an average value of 0.205 would reverse the increase in emission back to 1950 levels.

Re-radiation Increase

The values presented in Table 7 are for increase in LWR due to the UHI effect. However, some of LWR increase from the UHI effect is re-radiated back to Earth by GHGs compounding the UHI effect. Typical Earth energy budgets are about 240W/m^2 for LWR but the total warming is about 390 W/m^2. This is about 60% increase from the 240W/m^2 due to GHGs. Considering re-radiation; we can assume the UHI effect is actually creating an added increase by roughly a factor of 1.618 (refined from the planetary emissivity constant). Therefore the numbers can be adjusted accordingly when including re-radiation:

- Schneider nominal case from 1950 to 2019 including re-radiation (Row 8) yields 0.068W/m^2 and 0.183W/m^2 due to urban area and dome amplification coverage, respectively. These figures equate to about 1.9% and 5.1% of global warming assuming the total increase from 1950 is about 0.95°C in 2019.
- GRUMP worst-case from 1950 to 2019 including re-radiation yields 0.33W/m^2 and 0.87W/m^2 due to urban area and dome amplification coverage, respectively. This roughly equates to 9.2 and 24% of global warming assuming the total increase from 1950 is about 0.95°C in 2019.

Although global warming assessment obtained in the WAASU model, especially for the Schneider case does not appear to show much contribution to global warming, when contributions to climate feedback estimates are included, they show increased significance. Examples are provided in Appendix C that helps to demonstrate that when we include these feedback contributions to global warming, the UHI effect is responsible for as much as 7.3% in the Schneider case and up to 27% for the GRUMP case (see Table C4).

Table 7. Albedo and radiative increase model results with UHI effective area.

Year	Urban Extent Global Area %	UHI AEA % Area	UHI Normalized EAA Global Surface %Area	Albedo Cities	Global Weighted Albedo	ΔP_α UHI Radiative Increase W/m^2 (%GW)*	Re-radiation ΔP_α x1.618 UHI Radiative Increase W/m^2 (%GWx1.618)*	Area Forcing $\frac{\Delta P_\alpha\,(W/m^2)}{\%NAAA}1.618$ $\left(\frac{\Delta P_\alpha\,(W/m^2)1.618}{\Delta Global\ Albedo}\right)$
Nominal Case Schneider Study								
1950	0.059	0.059	0.059	0.12	29.4118	0	0	—
2019	0.188	0.459 (Area AF)	0.457	0.12	29.3994	0.0422 (1.18%)*	0.0683 (1.9%)	0.149 (5.5)
2019	0.188	1.143 (Dome AF)	1.1307	0.12	29.3786	0.113 (3.16%)*	0.1827 (5.11%)	0.162 (5.22)
What if	0.188	0.459, 1.58 (Area-Dome AF)	0.457, 1.13	0.202, 0.209	29.4118	-0.042 -1.129,	NA	—
Worst-Case GRUMP Study								
1950	0.316%	0.316	0.316	0.12	29.4118	0	0	—
2019	0.952%	2.288 (Area AF)	2.2437	0.12	29.3519	0.204 (5.7%)*	0.33 (9.22%)	0.147 (5.5)
2019	0.952%	5.658 (Dome AF)	5.395	0.12	29.2539	0.537 (15%)*	0.869 (24.3%)	0.162 (5.5)
What if	0.952%	2.288 5.658	2.2437 5.395	0.2009 0.2087	29.4118	-0.204 -0.537	NA	—

*Percent of Warming estimate, P_α=340 x (1-Albedo), %GW=$\{(P_\alpha/\sigma)^{0.25}_{2019} - (P_\alpha/\sigma)^{0.25}_{1950}\}(1.618)/0.95°C$,

4 Conclusions

In this paper, we were able to provide estimates of UHI effect (with urban areas) on global warming. This calculation was done with the aid of assumptions for area UHI amplification factors. These estimates inserted into our WAASU model found that between 0.042W/m^2 to 0.537W/m^2 of increase in LWR forcing is possible (this result indicates that about 1.9% to 24% of global warming may be due to the UHI effect including urban areas). This wide variation is due to both the amplification and urban area uncertainties. However, the model found that the effective UHI area **forcing** estimates were consistent and about 0.155W/m^2 per % of Normalized Effective Amplified Area. Re-radiation of this LWR change was estimated to increase the LWR forcing by a factor of 1.6. Examples are provided in Appendix C (see Table C4) to illustrate how the UHI assessment contributions can increase significantly when climate feedback problems are included. These estimates included global warming values due to the loss of sea ice over the last two decades in Appendix C; this also demonstrates the strength of the model. The final results were very dependent on UHI area estimates and amplification factors. Therefore, refined values of both would be important for future studies.

Below we provide suggestions and corrective actions which include:

- Albedo guidelines for both UHIs and roads similar to on-going CO_2 efforts.
- Guidelines for future albedo design considerations of cities.
- Recommend an agency like NASA to be tasked with finding applicable solutions to cool down UHIs.
- Recommendation for cars to be more reflective. Although world-wide vehicles likely do not embody much of the Earth's area, recommending that all new manufactured cars be higher in reflectivity (e.g., silver or white) would help raise awareness of this issue similar to electric automobiles that help improve CO2 emissions.

Appendix A: Growth Rates and Information on Natural Aggregates

Below is a plot of the world population growth rate that varies from about 2.1% to 1.1%. This graph is used to make growth rate estimates of urban coverage. We note that natural aggregates used to build cities and roads are reasonably correlated to population growth in Figure A2a. Also of interest (Fig. A2b) is the fact that one can see some correlation to global warming with the use of natural aggregates.

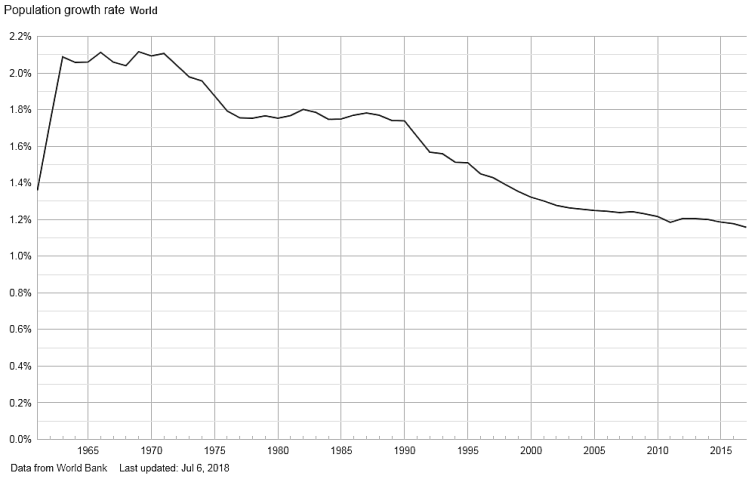

Figure A1. Population growth rate by year from 1960 to 2018, World Bank, [26]

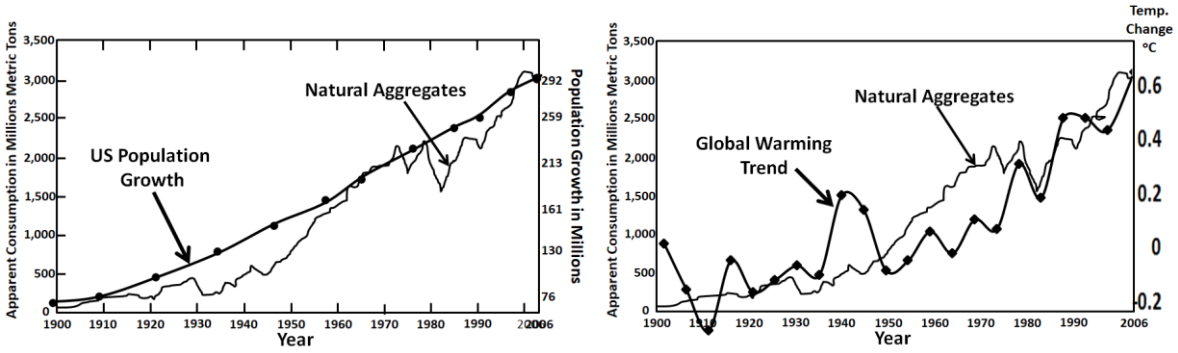

Figure A2. a) Natural aggregates [27] correlated to U.S. Population Growth (USGS [28]) **b)** Natural aggregates [27] correlated to global warming (NASA [29])

Appendix B: Albedo Model Normalization Information

Table 5a is reproduced from above, while Table 5b is the results of the Schneider dome area case. The results is used to demonstrate how normalization is performed

Table B1. Schneider results (Albedo=29.4118, 1950)

Surface	Albedo	% Area of Surface	Normalized Earth Area	Weighted Albedo %
	A	B	C=A x B x (1-0.67)	A x C
Sum of Water Type		71		
Sea Ice	0.6	15	4.95	2.970
Water	0.06	56	18.48	1.109
Sum of Land		29		

Table B2. Schneider results (Albedo=29.3786%, 2019)

Surface	Albedo	Normalized % Surface Area	Normalized Earth Area	Weighted Albedo %
	A	B	C=A x B x (1-0.67)	A x C
Sum of Water Type		70.239		
Sea Ice	0.6	14.839	4.897	2.938
Water	0.06	55.4	18.282	1.097
Sum of Land		29.761		

Type				
Land - (UHI + Coverage)	0.3118	28.941	9.55053	2.978
UHI + Coverage	0.12	0.059	0.01947	0.002
		∑=100.000	33.000	7.05882
			Cloud Area	
Clouds	0.3336	67	67	22.35294
∑ Sum Earth %			100.000	
∑ Global Albedo				29.4118

Type				
Land - (UHI + Coverage)	0.3118	28.631	9.448	2.946
UHI + Coverage	0.12	1.1307	0.373	0.0447757
		∑=100.000	33.000	6.980769
			Cloud Area	
Clouds	0.3336	67	67	22.3530
∑ Sum Earth %			100.000	
∑ Global Albedo				29.3786

Normalization is done as follows:

1. Model starts with 1950 Table 5a albedo 29.4118%, then 2019 urban coverage area is entered.
2. For example, in Table B1, the new area increases from 0.059% to 1.143%. This value is 1.084% larger, now the 'Sum of % of Earth Area' will be 101.084% in 2019.
3. All areas are renormalized to 101.084%. For example, sea ice at 15% in 1950 becomes 15%x(100.000/101.084)= 14.839% and the Urban Coverage becomes 1.143%x(100/101.084)=1.1307%.

Appendix C: Related Warming Estimates and Other Amplification Factors

Although the results obtained here at first seem to indicate that UHIs do not appear to contribute much to global warming, when the contributions of the UHI effect to the global warming feedback problem is included, much stronger significance can be estimated. In this appendix, feedback is assessed providing a number of global warming estimates.

- ***Such estimates are difficult to accurately calculate; however, it is not uncommon to look at how factors affect each other in climate science. Therefore, we have chosen to provide these in this appendix mainly as an aid for the reader to illustrate how climate sensitivity can factor into the magnitude of UHIs warming significance. These estimates should be considered only as rough approximate values.***

C.1 Global Feedback Amplification Factors

There is a wide range for possible estimates of climate feedback driven by uncertainties in how water-vapor, clouds, and other factors change as the Earth warms. Climate feedbacks are mixed and some will amplify (positive feedback) or diminish the effect of warming from the root-cause effects (for example see Hausfather [30]). The actual feedback is known to be positive (van Nes [31]). Climatologists will often approximate such factors frequently in reference to CO_2 doubling theory as positive. For example, water-vapor feedback alone, which is one of the most important in our climate system, is thought to have the capacity to approximately double the direct warming (Manabe and Wetherald [32], Randall et al [33], Dessler et. al [34]). This effect results from the fact that warm air holds more greenhouse moisture gas. Climate models incorporate this feedback. Water-vapor feedback is strongly positive, with most evidence supporting a magnitude of 1.6 to 2.0 $W/m^2/K$ (Dessler et. al. [34]). Also water-vapor feedback is considered a faster feedback mechanism (Hansen [35]). We will use a factor of 1.75, a bit less than a doubling factor of 2. This factor would apply equally to UHI warming contribution, Greenhouse Gases (GHG), or warming due to sea ice melting.

C.2 Weighted Albedo Solar Model Applied to the Melting of Sea Ice

We need to make a number of initial estimates in order to obtain a ballpark number of the warming due to sea ice loss. The first estimate is that the Antarctic sea ice has remained roughly constant (NOAA, Scott [36]) over the last two decades. Next we note that the Antarctic sea ice is larger in the winter while the Arctic sea ice is much larger in the summer. The difference appears to yield an estimate that the Arctic sea ice area is about 60% larger on average compared with Antarctic sea ice areas on a yearly basis (NOAA, Scott [36]). It has been observed that the Arctic sea ice is melting at an alarming rate of 12.85% in the last two decades (NASA sea ice [37]). This apparent trend appears to yield an estimated 26% decrease in sea ice in the last two decades. It is difficult to find a strong reference for quantifying global warming impact due to Arctic sea ice melting. However, we can get an approximation using a similar Weighted Albedo Solar (WAS) model (and also illustrate the strengths of these models). Sea ice melting will result in a significant albedo change that roughly changes the ice albedo of 0.6, to the open ocean albedo of 0.06 (see Table C1 and C2). Fortunately, the Arctic areas receive only about 40% as much solar radiation (Sciencing [38])

reducing the feedback effect. From Equation 6, the effective sea ice surface area reduction from the irradiance decrease can be approximated as

Effective sea ice surface area= 0.6 x 15% (1-0.26 x 0.40)=8.06% (a 0.94% reduction of effective area). (C-1)

Here 0.6 x 15% is sea ice percent in Arctic area, 0.26 is the fraction of sea ice lost, and 40% is the solar irradiance effect. In the WAS model, we will have to make an assumption that the effective ocean surface area increases proportionately by 0.94% to 56.94% (see Table C2). The model then finds that the global albedo change decreases from 29.4118% to 29.2443%. (Note that alternately we could have set the albedo to 29.4118% in 2019 and worked back to 1950. In this case the albedo would have increased to 29.2443%).

The percent Global Warming (GW) is found as:

$$\%GW=\{(P/\varepsilon\sigma)^{0.25}{}_{2019}- (P/\varepsilon\sigma)^{0.25}{}_{1950}\}/0.95^{o}C, \quad \text{(C-2)}$$

where P=340W/m^2 x (1-Albedo) and ε=1. The warming increase due to ice melting is estimated from this model to be about 0.15^{o}C or 15.8% of the 0.95^{o}C increase in 2019. The increase in radiative forcing is 0.6 W/m^2. The feedback is then roughly 0.63 W/m^2/^{o}K where we assume a temperature change of 0.95^{o}C over this time period.

These values should only be taken as a rough estimate due to numerous uncertainties as climatologists find it hard to fully quantify the seasonal variations in ice change and to know the possible impact on cloud coverage increase from additional warming evaporation. However, one would expect less evaporation in the Arctic. Thus, there are a lot of uncertainties.

Table C1. Schneider results (Albedo=29.4118, 1950)

Surface	Albedo	% Area of Surface	Normalized Earth Area	Weighted Albedo %
	A	B	C=A x B x (1-0.67)	A x C
Sum of Water Type		71		
Sea Ice	0.6	15	4.95	2.970
Water	0.06	56	18.48	1.109
155Sum of Land Type		29		
Land - (UHI + Coverage)	0.3118	28.941	9.55053	2.978
UHI + Coverage	0.12	0.059	0.01947	0.002
		∑=100.000	33.000	7.05882
			Cloud Area	
Clouds	0.3336	67	67	22.35294
∑ Sum Earth %			100.000	
∑ Global Albedo				29.4118

Table C2. Sea ice loss - albedo change (29.0643%, 2019)

Surface	Albedo	Normalized % Surface Area	Normalized Earth Area	Weighted Albedo %
	A	B	C=A x B x (1-0.67)	A x C
Sum of Water Type		71		
Sea Ice	0.6	14.06	4.4352	2.507
Water	0.06	56.94	18.9948	1.14
Sum of Land Type		29	23.43	
Land - (UHI + Coverage)	0.3118	28.941	9.55053	2.978
UHI + Coverage	0.12	0.059	0.01947	0.002
		100.000	33.000	6.6395
			Cloud Area	
Clouds	0.3336	67	67	22.3530
∑ Sum Earth %			123.430	
∑ Global Albedo				29.2443

C.3 Estimated Contributions to Global Warming

Table C3 summarizes the key global warming cause and effect factors that we have described.

Table C3. Global warming factors of interest

Urban Climate Amplification	Effects	Where Applied
UHI Area Amplification Factor	3.1 UHI Amplification	Applied to 2019 UHI Area
UHI Dome Horizontal Method	2.9 UHI Amplification	Applied to 2019 UHI Area
Ice Melting	0.15^{o}C	0.15 ^{o}C out of 0.95 ^{o}C
Atmospheric Moisture Increase	1.75 GW Amplification	Applied to Ice Melting Temp, UHI, and GHGs +X*

where X is any other feedbacks (positive or negative)

Then major contributions to global warming can be simplified as follows for the 2019 warming trend

$$\Delta T_{GW} = \Delta T_{UHI} + \Delta T_{Water-Vapor} + \Delta T_{Sea-Ice} + \Delta T_{GHG} + \Delta T_{X}, \quad \text{(C-3)}$$

where ΔT_{GW}=0.95°C, $\Delta T_{UHI\text{-}Schneider}$=0.018°C (Table 7, 1.9%x0.95°C), and $\Delta T_{Sea\text{-}Ice}$=0.15 °C. We have three unknowns $\Delta T_{Water\text{-}Vapor}$, ΔT_{GHG} and ΔT_X. Here X is for all other feedback temperature rise due to lapse rate and increases in cloud coverage and so forth. Therefore, this value can be effectively either positive or negative. The following two equations will help in obtaining some estimates:

$$0.95^oC = AF_{water\ vapor}(\Delta T_{UHI} + \Delta T_{GHG}) + \Delta T_x + \Delta T_{Sea\text{-}Ice} = 1.75\ (0.018\ ^oC + \Delta T_{GHG}) + \Delta T_x + 0.15\ ^oC \quad \text{(C-4)}$$

and

$$0.95^oC = \Delta T_{UHI} + \Delta T_{GHG+X} + \Delta T_{Sea\text{-}Ice} + \Delta T_{Water\text{-}Vapor} = 0.018\ ^oC + \Delta T_{GHG+X} + 0.15\ ^oC + \Delta T_{Water\text{-}Vapor.} \quad \text{(C-5)}$$

To obtain some example values, we need to make an assumption since we have two equations and three unknowns. We will assume that T_{GHG} is 40% of global warming so that ΔT_{GHG}=0.38°C. Using this estimate, with the water-vapor $AF_{water\text{-}vapor}$=1.75 discussed above, and equations C-4 and C5, we can obtain examples of the other temperature rises due to feedbacks. These examples are provided in Table C4 for the UHI effect variations.

These examples illustrate the UHI effective (and urban coverage) contributions to Global Warming (GW) that occur when feedback problems are included showing this range between 2.9 to 27%.

From the table, we note UHI effective temperature rise feedback contribution factor increase of 2.43 (2.87%/1.18%), 2.3 (7.32%/3.16%), 2.2 (12.5%/5.7%), and 1.8 (27.3%/15%) with an average value of 2.2. Using this average value, it indicates that the UHI area feedback contribution could increase from 0.096W/m^2/% to about 0.21W/m^2/% Normalized Effective Amplified Area (see Table 7). Although these values are crude estimates, they serve as possible helpful examples.

Schneider Temp

Table C4. Global warming contributions (2019)

Warming Component	**Temperature Contribution (°C)**	**GW Percent Root-Cause Contribution* (Re-radiation)†**	**Percent of GW**	**Temperature Contribution (°C)**	**GW Percent Root-Cause Contribution* (Re-radiation)†**	**Percent of GW**
	Schneider Study UHI Area Amplification=3.1			UHI Dome Amplification=8.4		
Urbanization ΔT	**0.018**	~~2.87~~ (4.5)	1.18%	**0.0485**	~~7.32~~ (11.3)	3.16%
Greenhouse gases (40%) ΔT	0.38	~~97.13~~ (95.5)	40.0%	0.38	~~92.68~~ (88.7)	40.00%
Sea ice melt feedback ΔT- rise	**0.15**		**15.8%**	**0.15**		**15.8%**
Water-vapor feedback ΔT- rise	0.4		41.5%	0.426		43.2%
X (Other) ΔT	0.0018		1.51%	-0.054		-2.14%
Total	**∑0.95**			**∑0.95**		
	GRUMP Study UHI Area Amplification=3.1			UHI Dome Amplification=8.4		
Urbanization ΔT	**0.0876**	**~~12.47~~ (18.7)**	**5.70%**	0.23	**~~27.27~~ (37.8)**	**15.00%**
Greenhouse gases (35%) ΔT	0.38	~~87.53~~ (81.3)	40%	0.38	~~72.73~~ (62.2)	40.00%
Sea ice melt feedback ΔT- rise	0.15		15.8%	0.15		15.8%
Water-vapor feedback ΔT-rise	0.459		45.3%	0.579		53.2%
X (Other) ΔT	-0.126		-6.82%	-0.39		-23.95%
Total	**∑0.95**			**∑0.95**		

* $\%\Delta T_{GHG} = \Delta T_{GHG}/(\Delta T_{GHG} + \Delta T_{Urbanization})$ and $\%\Delta T_{Urbanization} = \%\Delta T_{Urbanization}/(\Delta T_{GHG} + \Delta T_{Urbanization})$, † Considering a 1.618 re-radiation factor for the UHI effect from GHGs

Note that the actual radiative forcing and feedback parameters are not listed but could be estimated utilizing the plank's λ_o feedback parameter and the associated temperature rises of interest in the table.

Appendix D: WAASU Model References

Table D1 provides references for the WAASU model values.

Table D1 Key References for WAASU model

Parameter	Albedo References	1950 Area References
Sea Ice	50-70%, average 60% (NSID [39])	15% (Lindsey [40])
Water	6% (NSID [39])	56% Ocean+Sea Ice=71% (USGS [41])
Land-(UHI+Coverage)	Adjusted to obtain 29.412% and surface reflected of 7.06 Earth Albedo in 1950 thereafter held fixed (see IPCC Hartmann [13] AR5 report)	29%-Urban Coverage
UHI+Cov	0.12 Sugawara et. Al [41]	See Table 1
Clouds	22.35294 (IPCC Hartmann et al. [13])	67% (Earthobservatory, NASA [42])
Earth Albedo	29.412% (IPCC Hartmann [13])	-

Conflicts of Interest

The author declares that he has no conflicts of interest.

References

1 McKitrick R. and Michaels J. 2004. A Test of Corrections for Extraneous Signals in Gridded Surface Temperature Data, Climate Research

2 McKitrick R., Michaels P. 2007 Quantifying the influence of anthropogenic surface processes and inhomogeneities on gridded global climate data, J. of Geophysical Research-Atmospheres. Also see McKitrick Website Describing controversy: https://www.rossmckitrick.com/temperature-data-quality.html

3 Schmidt G. A. 2009 Spurious correlations between recent warming and indices of local economic activity, *Int. J. of Climatology*

4 Zhao, Z.-C., 1991: Temperature change in China for the last 39 years and urban effects. Meteorological Monthly (in Chinese), 17(4), 14-17.

5 Feddema, J. J., K. W. Oleson, G. B. Bonan, L. O. Mearns, L. E. Buja, G. A. Meehl, and W. M. Washington (2005), The importance of land-cover change in simulating future climates, *Science*, 310, 1674– 1678, doi:10.1126/science.1118160

6 Ren, G.; Chu, Z.; Chen, Z.; Ren, Y. 2007 Implications of temporal change in urban heat island intensity observed at Beijing and Wuhan stations. *Geophys. Res. Lett.* , *34,* L05711,doi:10.1029/2006GL027927.

7 Ren, G.-Y., Z.-Y. Chu, J.-X. Zhou, et al., (2008): Urbanization effects on observed surface air temperature in North China. J. Climate, 21, 1333-1348

8 Jones, P. D., D. H. Lister, and Q.-X. Li, 2008: Urbanization effects in large-scale temperature records, with an emphasis on China. J. Geophys. Res., 113, D16122, doi: 10.1029/2008JD009916.

9 Stone B. 2009 Land use as climate change mitigation, Environ. Sci. Technol., 43(24), 9052– 9056, doi:10.1021/es902150g

10 Zhao, Z.-C., 2011: Impacts of urbanization on climate change. in: 10,000 Scientific Difficult Problems: Earth Science, 10,000 scientific difficult problems Earth Science Committee Eds., Science Press, 843-846. 30%

11 Yang, X.; Hou, Y.; Chen, B. 2011 Observed surface warming induced by urbanization in east China. *J. Geophys. Res. Atmos*, 116, doi:10.1029/2010JD015452.

12 Huang Q. , Lu Y. 2015 Effect of Urban Heat Island on Climate Warming in the Yangtze River Delta Urban Agglomeration in China, *Intern. J. of Environmental Research and Public Health* 12 (8): 8773 (30%)

13 Hartmann, D.L., A.M.G. Klein Tank, M. Rusticucci, L.V. Alexander, S. Brönnimann, Y. Charabi, F.J. Dentener, E.J. Dlugokencky, D.R. Easterling, A. Kaplan, B.J. Soden, P.W. Thorne, M. Wild and P.M. Zhai, 2013: Observations: Atmosphere and Surface. In: Climate Change 2013: The Physical Science Basis. Contribution of Working Group I to the Fifth Assessment Report of the Intergovernmental Panel on Climate Change [Stocker, T.F., D. Qin, G.-K. Plattner, M. Tignor, S.K. Allen, J. Boschung, A. Nauels, Y. Xia, V. Bex and P.M. Midgley (eds.)]. Cambridge University Press, Cambridge, United Kingdom and New York, NY, USA.

14 Satterthwaite D.E., F. Aragón-Durand, J. Corfee-Morlot, R.B.R. Kiunsi, M. Pelling, D.C. Roberts, and W. Solecki, 2014: Urban areas. In: Climate Change 2014: Impacts, Adaptation, and Vulnerability. Part A: Global and Sectoral Aspects. Contribution of Working Group II to the Fifth Assessment Report of the Intergovernmental Panel on Climate Change (IPCC)

15 Schneider,A., M. Friedl, and D. Potere, 2009:A new map of global urban extent from MODIS satellite data. Environmental Research Letters, 4(4), 044003, doi:10.1088/ 1748-9326/4/4/044003

16 Global Rural Urban Mapping Project (GRUMP) 2005, Columbia University Socioeconomic Data and Applications Center, Gridded Population of the World and the Global Rural-Urban Mapping Project (GRUMP).

17 NASA 2000, Gridded population of the world, , https://sedac.ciesin.columbia.edu/data/set/gpw-v3-

population-count/data-download

18 Galka M. 2016, Half the World Lives on 1% of Its Land, Mapped, https://www.citylab.com/equity/2016/01/half-earth-world-population-land-map/422748/, , (2016 publication on 2000 data set, http://metrocosm.com/world-population-split-in-half-map/

19 Zhou Y. , SmithS. , Zhao K. , M. Imhoff, A. Thomson, B. Lamberty,G. Asrar, X. Zhang, C. He and C. Elvidge, A global map of urban extent from nightlights, Env. Research Letters, 10 (2015), (study uses a 2000 data set).

20 Zhao L, Lee X, Smith RB, Oleson K, 2014, Strong, contributions of local background climate to urban heat islands, Nature. 10;511(7508):216-9. doi: 10.1038/nature13462

21 Basara J. ,P. Hall Jr. , A.Schroeder , B.Illston ,K.Nemunaitis 2008, Diurnal cycle of the Oklahoma City urban heat island, J. of Geophysical Research

22 Barr J. M., 2019 The Economics of Skyscraper Height (Part IV): Construction Costs Around the World, https://buildingtheskyline.org/skyscraper-height-iv/

23 Zhang, X., Friedl, M. A., Schaaf, C. B., Strahler, A. H. & Schneider, A. 2004 The footprint of urban climates on vegetation phenology. *Geophys. Res. Lett. 31, L12209*

24 Zhou D. , Zhao S. , L. Zhang, G Sun and Y. Liu, 2015, The footprint of urban heat island effect in China, *Scientific Reports*. 5: 11160

25 Fan, Y., Li, Y., Bejan, A. *et al.* Horizontal extent of the urban heat dome flow. *Sci Rep* 7, 11681 (2017). https://doi.org/10.1038/s41598-017-09917-4

26 World Bank, 2018 population growth rate, worldbank.org

27 USGS 1900-2006, Materials in Use in U.S. Interstate Highways, https://pubs.usgs.gov/fs/2006/3127/2006-3127.pdf

28 US Population Growth 1900-2006, u-s-history.com/pages/h980.html1

29 NASA 1900-2006 updated, 2020 https://climate.nasa.gov/vital-signs/global-temperature/

30 *Hausfather Z., (2018) How Scientist Estimate Climate Sensitivity, in Carbon Brief,* https://www.carbonbrief.org/explainer-how-scientists-estimate-climate-sensitivity

31 van Nes E. H., Scheffer M., Brovkin V., Lenton T. M., Ye H, Deyle E. and Sugihara G., Nature Climate Change 2015. dx.doi.org/10.1038/nclimate2568

32 Manabe, S., and R. T. Wetherald (1967), Thermal equilibrium of atmosphere with a given distribution of relative humidity, J. Atmos. Sci., 24, 241–259.

33 Randall, D. A.et al. (2007), Climate models and their evaluation, in Climate Change 2007: The Physical Science Basis. Contributions of Working Group I to the Fourth Assessment Report of the Intergovernmental Panel on Climate Change, edited by S. Solomon et al., pp. 591–662, Cambridge Univ. Press, Cambridge, U.K.

34 Dessler A. E. ,Zhang Z., Yang P., Water-vapor climate feedback inferred from climate fluctuations, 2003–2008, *Geophysical Research Letters*, (2008), https://doi.org/10.1029/2008GL035333

35 Hansen, J., "2008: Tipping point: Perspective of a climatologist." Archived 2011-10-22 at the Wayback Machine, Wildlife Conservation Society/Island Press, 2008. Retrieved 2010.

36 NOAA, Scott, M, 2019, Understanding Climate:Antarctic sea ice extent, https://www.climate.gov/print/833949

37 NASA Sea Ice, 2019, https://climate.nasa.gov/vital-signs/arctic-sea-ice/

38 Sciencing (2018) https://sciencing.com/sun-intensity-vs-angle-23529.html

39 NSID 2020, National Snow & Ice Data Center, "Thermodynamics: Albedo". nsidc.org. Retrieved 14 August 2016. https://nsidc.org/cryosphere/seaice/processes/albedo.html

40 Lindsey R, Scott M., (2019), Climate Change: Arctic Sea Ice Summer Minimum, NOAA Climate.gov, https://www.climate.gov/news-features/understanding-climate/climate-change-minimum-arctic-sea-ice-extent

41 Sugawara, H., Takamura, T. Surface Albedo in Cities (0.12): Case Study in Sapporo and Tokyo, Japan. *Boundary-Layer Meteorol* 153, 539–553 (2014). https://doi.org/10.1007/s10546-014-9952-0

41 USGS on Amount of Earth covered by water, https://www.usgs.gov/special-topic/water-science-school/science/how-much-water-there-earth?qt-science_center_objects=0#qt-science_center_objects

42 Earthobservatory, NASA (clouds albedo 0.67) https://earthobservatory.nasa.gov/images/85843/cloudy-earth